Research Article

Journal of Chemistry: Education Research and Practice

Adsorptive Potential of Acid Modified Moringa Oleifera Wastes for Tannery Effluent Decontamination

Wombo NP[1,2], Itodo AU[2]*, Wuana RA[2] and Charles O Oseghale[1]

[1]*Department of Chemistry, Federal University of Agriculture, Makurdi, Nigeria*

[2]*Department of Chemistry, Federal University Lafia, Nigeria*

***Corresponding author**
Dr. A.U. Itodo (MCSN, MICCON), Department of Chemistry, Federal University of Agriculture, Makurdi, Nigeria, Tel: +234-8039503463; E-mail: itodoson2002@gmail.com

Submitted: 20 Dec 2017; **Accepted**: 28 Dec 2017; **Published**: 19 Jan 2018

Abstract

Removal of chromium from tannery effluent was carried out using low-cost adsorbents derived from Moringa oleifera seed shells and pods adsorbents. The precursor was modified using acid (H_2SO_4) impregnation method and characterized using CHNO/S elemental analyzer, FT-IR, SEM, TEM and PXRD. Physicochemical study of the tannery effluent was carried out and documented. Result shows that most physico-chemical parameters investigated for the effluent are above the permissible limit outlined by WHO. Initial concentration of the pollutant, Chromium (987 mg/L) exceeds WHO limit. The maximum adsorption capacity of AMMOS was found to be 137.4 mg/g and that of AMMOP was 277.3 mg/g for chromium removal. Column adsorption study was used to study the effect of experimental variables (pH, initial adsorbate concentration, contact time, adsorbent dosage and temperature), while RE% of Cr by the adsorbents was calculated and recorded for all experimental runs. The equilibrium study for the sorption of Cr was investigated using the Langmuir, Freundlich, Dubinin-Radushkevich and Temkin isotherm model. The linearity of the respective models include: Langmuir (R^2 of 0.271 for AMMOP and 0.7661 for AMMOS), Freundlich R^2 values for AMMOS (0.8337) and AMMOP (0.6485) thus, presenting the Freundlich model as the most applicable isotherm model. Temkin and Dubinin-Radushkevich isotherm models gave poor fittings for Cr on the adsorbents. The rate and mode of diffusion is best explained using the Pseudo-second order kinetic and film diffusion respectively suggesting that the kinetics of the sorption process is controlled by diffusion through the liquid film surrounding the solid sorbent. The efficiency in remediation of effluent using the adsorbents as compared with commercial activated carbon at 95% confidence interval shows that there is no significant difference. This implied that the used of Moringa oleifera seed shells and pods for adsorbents is an economically viable approach to combat remediation challenges in the removal of Chromium from Tan chrome liquor.

Introduction

The production of leather, leather goods, leather boards and fur produces numerous by products, solid wastes, high amounts of wastewater containing different loads of pollutants and emissions into the soil and air. The uncontrolled release of tannery effluents to natural water bodies increases health risks for human beings and environmental pollution. Effluents from raw hide processing tanneries, which produce wet blue, crust leather or finished leather, contain compounds of trivalent chromium (Cr) and sulphides in most cases. Organic and other ingredients are responsible for high BOD (biological oxygen demand) and COD (chemical oxygen demand) values and represent an immense pollution load, causing technical problems, sophisticated technologies and high costs in concern with effluent treatment [1]. Contamination of tannery waste water with organics and inorganics is a matter of concern, because of their harmful effects on living organisms. Adsorption process is superior to any other method by virtue of its low initial cost, low energy requirement, simplicity of design and possibility of reusing the spent carbon via regeneration. Adsorbent such as activated carbon available to remove organic compounds from wastewaters are costly and hardly available [2,3]. Base on this, there is a need to study the effectiveness of uptake of pollutants from tanneries by considering cost effectiveness, availability and favorable adsorptive properties.

Moringa oleifera tree (drumstick tree) is a rapid growing deciduous shrub or small tree of about 13 m tall and 35 cm in diameter with an umbrella-shaped open cap [4-6]. Moringa oleifera is the most widely distributed species of the Moringaceae family throughout the World [7, 8]. It has also been reported that Moringa oleifera oil and micronutrients contain antitumor, antiepileptic, antidiuretic, anti-inflammatory and venomous bite characters [9]. Moringa oleifera contains specific plant pigments with demonstrated powerful anti-

oxidative ability such as vitamins C, E, A, caffe-oylquinic acids, carotenoids-lutein, alpha-carotene and beta carotene, kaempferol, quercetin, rutin [10-12].

The numerous nutritional and medicinal uses of this plant are quite alarming, notwithstanding, conversion of its residues (e.g. seed pod and seed shells), are still under optimized.

In this study, we report the peparation and characterization of acid modified Moringa Oleifera shells and pods adsorbents and studied the adsorptive properties in column mode experiment of the removal of Cr (IV) from tannery effluents.

Materials and Methods

A CHNS/O microanalyser (Perkin-Elmer 240C series, USA) elemental analyzer was used for elemental analysis. The infrared spectra profile was performed using a SHIMADZU 8400C, (Japan). Powder X-ray diffraction (PXRD) patterns were recorded on a BRUKER -AXS D8 Advanced X-ray Diffractometer (Germany) with Cu-Kα radiation machine at the Department of Chemistry, University of York, United Kingdom. The X- ray diffraction data were recorded using Cu Kα radiation (1.5406 A0). The relative intensity data were collected over a 2θ range of 10-40°C. Transmission Electron Micrograph (TEM) measurements were performed on a JEOL 1010 instruments (Japan) at 200 kV. These images were processed using an Image J (1.42q) software to obtain the particle size. The scanning electron micrographs (SEM), were performed on a Hitachi S-4800 microscope (Japan) at a voltage of 15 Kv. A T-60 UV-visible spectrophotometer (USA) at a resolution of 1 nm, was used to monitor the wavelength range between 200-800 nm. The chromium concentration was determined using A Zeenit 700 absorption spectrometer (Germany) coupled with a flame atomizer and a chromium hollow cathode lamp. AROSTEK Instrument column chromatography was used for the column studies. It has a diameter of 9-10 mm with a maximum loading capacity of 0.1 g.

Study Area

The tannery effluent was collected from Nigerian Institute of Leather and Science Technology (NILEST), an Institution of higher learning in Samaru-Zaria with coordinates; Latitude 11.1667^0, Longitude 7.6333^0.

Sampling

Sampling method documented by Itodo et al. was carefully followed. The effluent preservation method adopted was as described [13]. The effluent was analyzed for physicochemical parameters including: pH, temperature, Electrical conductivity and salinity. Determination of total solids (TS) Total dissolved solids (TDS), Total suspended solids (TSS), Chemical oxygen demand (COD) Measurement and Biochemical oxygen demand (BOD) measurements.

The precursor; Moringa oleifera seeds were obtained from the Central Market in Lafia, North central Nigeria. The Moringa oleifera seeds pods and shells were presented for identification at the Botany Department of the University of Agriculture Makurdi, Nigeria.

Preparation and Characterization of Adsorbents

The Moringa oleifera seed pods were de-seeded, de-shelled and washed with water to remove dust, sand and allowed to dry under room temperature. The seed pod were pounded and further blended to a coarse size (2 mm diameter).The prepared Moringa oleifera seeds pods and shells were chemically modified and coded as AMMOS (Acid Modified Moringa Oleifera Shell) and AMMOP (Acid Modified Moringa Oleifera Pods). The adsorbent pH was determined [14]. Method by Ahmedna et al. was used to determine the bulk density [15]. Attrition was determined by a procedure described by Toles et al, [16]. Adsorbent particle size was determined using image J on TEM images. The surface area was determined by the iodine adsorption test [17]. Fourier transformed infrared (FTIR), TEM, SEM, CHNO/S analysis were performed according to the manufacturer's instructions.

Column Adsorption Experiments

Column adsorption experiment was used to determine the removal of Cr from the tannery effluent. The method according to Ramuthai et al. was adopted. The adsorbents were packed into the vertical column to obtain the bed depth, and the column was tapped to remove air bubbles. The applied shaking (1000 rpm) speed allowed all the surface area to come in contact with heavy metal ions over the course of the experiments. All experiments were carried out in duplicate. The effect of various parameters on the rate of adsorption process was observed by varying contact time (20, 40, 60, 80and 100 min), adsorbate concentration (200, 400, 600, 800, and 1000 mg/L), temperature (10, 20, 30, 40, and 50°C), adsorbent dosage (0.01, 0.02, 0.03, 0.04, 0.05 g) and pH 2, 4, 6, 8, and 10 of the solution. The solution volume was kept constant. The effluent was collected before and after adsorption, digested and measured using Atomic Adsorption Spectrophotometer (AAS).

In all column adsorption experiments, the amount of chromium adsorbed, Qe (mg/g) and removal efficiency, RE (%) were calculated using Equations (1) and (2), respectively:

$$Q_e\,(mg/g) = \frac{(C_o - C_e)v}{w} \quad (1)$$

$$RE\ (\%) = \frac{(C_o - C_e)x100}{C_O} \quad (2)$$

Where Co and Ce are the initial and residual phenol concentrations (mg/L), respectively, V is the aliquot of the tannery solution used (L); and w is the weight of adsorbent in grams (g) used for a particular column treatment.

Results and Discussion

Physicochemical Characteristics of Adsorbents

Some physicochemical characteristics of the adsorbents are recorded in (Table 1).

A pH value of 7.28 and 7.24 was reported for AMMOP and AMMOS respectively after washing. These values are within the range recorded for activated carbons from olive stones and walnut shells [18]. The percentage yield of AMMOS is 24.65 and AMMOP is 23.75. Bulk densities (kg/m^3) for AMMOS and AMMOP were 24.65 and 23.75 respectively. These values are higher than the minimum requirement of 0.25 g/mL for adsorbent application in removal of pollutants from wastewater [19]. High attrition indicates that the adsorbents may be less effective and more expensive due to frequency of regeneration. More on attrition of adsorbent had been reported. Both adsorbents showed acceptable attrition after preparation.

Table 1: Physicochemical characteristics of adsorbents from Moringa oleifera seed shells and pod

S/No	Parameters	AMMOP	AMMOS
1	pH	7.28	7.24
2	Bulk density (g/cm^3)	24.65 ±0.02	23.75 ±0.02
3	Moisture contents (%)	6.84 ±0.02	6.14 ±0.02
4	Surface area (m^2/g)	181.17 ±0.02	170.13 ±0.02
5	Particle size (um)	38	36
6	Iodine adsorption number (x10^{-4} mol/g)	62.33 ±0.02	64.45 ±0.02

Bulk densities (kg/m^3) for AMMOS and AMMOP were 24.65 and 23.75 respectively. These values are higher than the minimum requirement of (0.25 g/mL) for application in removal of pollutants from wastewater [19]. The iodine number indicates the extent of micro-pore volume distribution within the adsorbents matrices, hence the surface area. Iodine numbers (x10^{-4} mol/g)/surface areas (m^2/g) were 62.33/118.17 and 64.45/170.13 for AMMOS and AMMOP, respectively. The surface areas are within the range (150 - 500 m^2/g) required for wastewater treatment and removal of small molecules from aqueous solutions [20].

Table 2: Physicochemical properties of the Tan-chrome Liquor

S/ NO	Parameters	Values	Permissible limits (WHO, date)
1	pH	8.14	5.5-9.0
2	Temperature	22.1	45.0
3	Odour	Offensive	
4	Colour (pt.co)	Brown	Light Permissible
5	Electric conductivity (mS)	1300	1200
6	Total hardness (mg/L)	333.33	-
7	Acidity (mg/L $CaCO_3$)	15	-
8	Alkalinity(mg/L $CaCO_3$)	225	-
9	Total solids (TS) (mg/L)	5.50	-
10	Total dissolved solids (TDS) (mg/L)	8250	2100
11	Total suspended solids (TSS) (mg/L)	1.8	-
12	Biochemical oxygen demands (BOD) (mg/L)	952	30
13	Chemical oxygen demands (COD) (mg/L)	1245	220

Physicochemical characterization of the tannery effluent was carried out parameters considered were; Electrical conductivity (1300), Biochemical oxygen demand (952); and chemical oxygen demand (1245), pH (8.14), Alkalinity (225), Acidity (15), Total hardness (333.33), Total dissolved solids (8250) and Total suspended solid (1.8) all parameters here are higher than permissible limits set as standards.

Table 3: Comparative elemental composition of adsorbents derived from Moringa seed pods

S/no	Parameters	AMMOS	AMMOP
1	Carbon (%)	6.12	4.88
2	Hydrogen (%)	6.02	5.02
3	Nitrogen (%)	12.11	8.11
4	Sulphur (%)	ND	ND
5	Oxygen (%)	10.22	10.22

ND- Not detected

Surface morphology

SEM Characterization

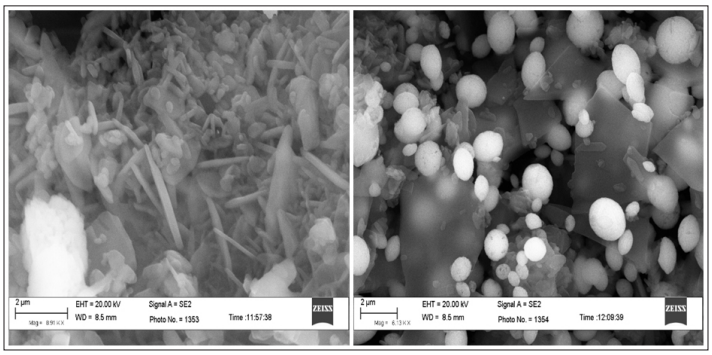

Plate 1: SEM images for AMMOS (LHS) and AMMOP(RHS)

FTIR Characterization

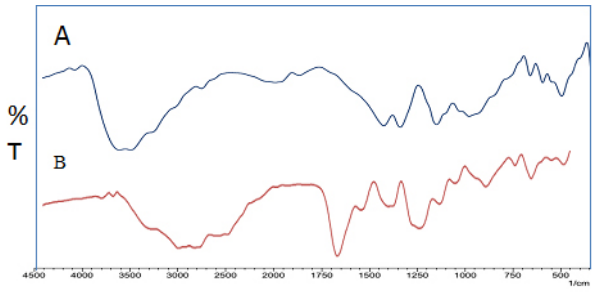

Figure 1: FT-IR Spectra of AMMOS (A) AMMOP (B)

Fourier transform infrared (FT-IR) spectroscopic analysis was used to study the surface chemistry of the surface modified Moringa oleifera seed pod and shell and functional groups. It can be seen from figure 1 that FT-IR spectra of the adsorbents have different frequencies. The FTIR spectra (Figure 1) of the adsorbents (AMMOS and AMMOP) showed broad bands at a range of 3446-3281 cm1 corresponding to -OH and -COOH stretching vibrational frequencies [21]. It was also observed that all the adsorbents falls under a group frequencies of 350-750 with functional groups of C-H; 750-1250 of C-O stretch, CH_2 symmetric deformation, N-N; 1250-1750 of N-N bend, C≡C stretch, C=C stretch; 1750-2500 of N=N=N anti symmetric stretch, C≡N, PH, C≡N; 2500-3500, O-H broad, O-N stretch, NH stretch, ≡CH-H stretch; 3500-4500 with a final group of O-H broad, O-H stretch, -NH stretch, ≡CH-H stretch [22]. These observed functional groups on the surface of the AMMOS and AMMOP indicated their similarities and the non destruction of the hydrocarbon and heteroatom surfaces.

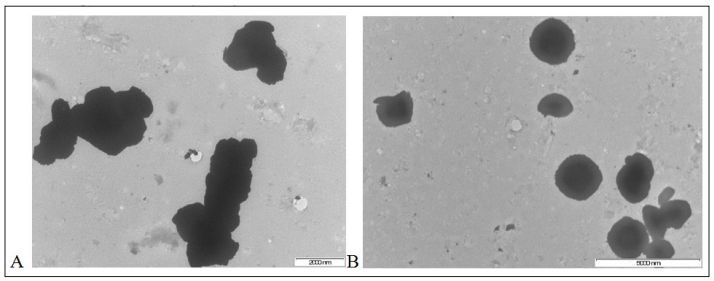

Plate 2: TEM images of AMMOS (A) and AMMOP (B)

The TEM image (Plate 2) revealed the small size of the adsorbents. The following particle size was observed for AMMOS (1.863584) and AMMOP (0.92837) using image J software on TEM particle distributions.

XRD Characterization

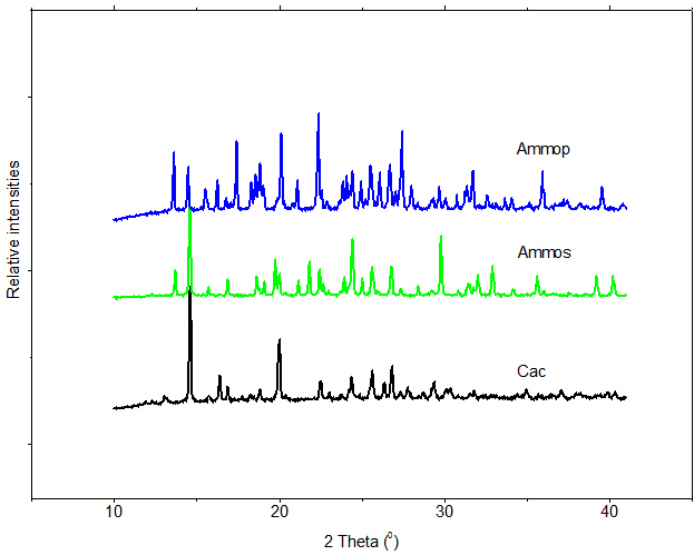

Figure 3: Comparison of PXRD pattern for AMMOP and AMMOS of the Adsorbents

X-ray diffraction (XRD) is a material characterization technique that can be useful for analyzing the lattice structure of a material. It investigates crystalline properties of a synthesized material. The XRD patterns of the adsorbents are presented in Figures 3. Low and high intensity Bragg diffraction peak were observed for the adsorbents. The XRD showed no peaks from impurities, indicating high purity of the adsorbents. The X-ray diffraction (XRD) analysis of AMMOS and AMMOP showed peaks that are amorphous in nature of biomass. The diffractograms also exhibits many significant peaks.

Effect of initial concentration on Chromium Removal

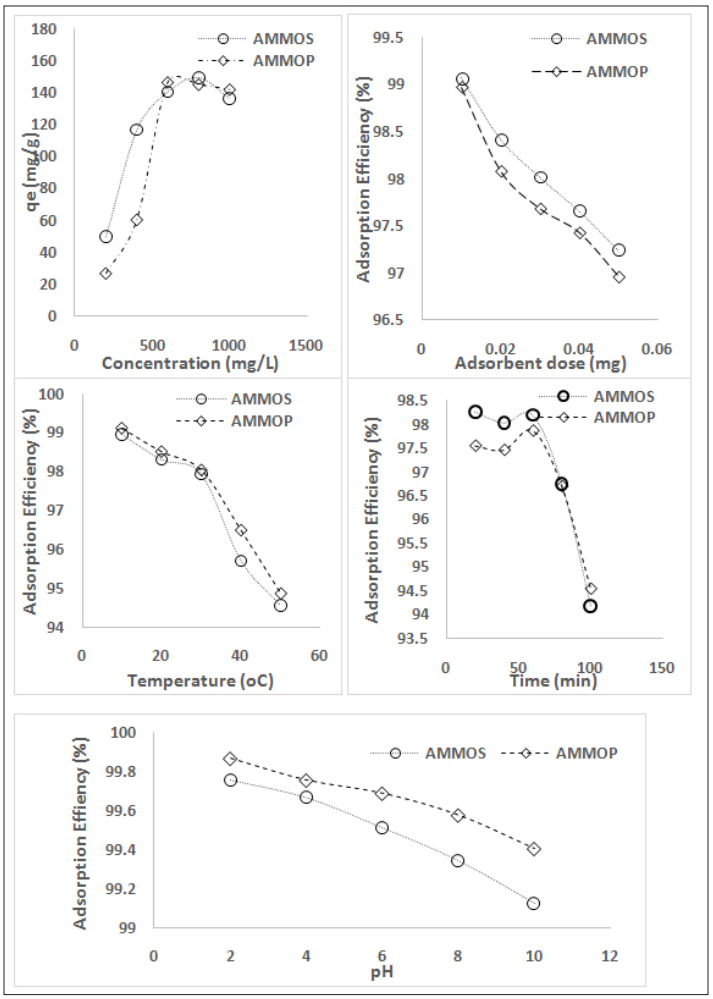

Figure 4: Effect of Initial concentration (a) temperature (b) time (c) pH (d) on Adsorption of chromium by acid modified Moringa oleifera seed (AMMOS) and pod (AMMOP)

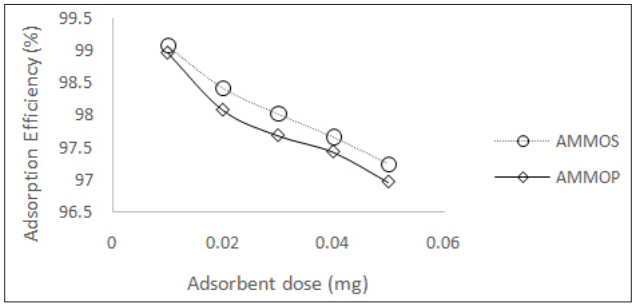

Figure 5: Effects of dosage on chromium removal by acid modified Moringa oleifera seed (AMMOS) and acid modified Moringaoleifera pod (AMMOP)

The adsorption capacity is influenced most by the pH of the solution. The pH of the solution primarily affects the surface charge of the adsorbents, degree of ionization, and speciation of chromium which may lead to change in equilibrium and kinetics chromium removal. The effect of initial solution pH (Figure 7) was investigated over the pH ranges of 2.0, 4.0, 6.0, 8.0, and 10.0 at a fixed initial concentration of chromium (25 mg/L). Theamount of phenol adsorbed decreased with increase in pH for both adsorbents. The highest chromium

uptake for AMMOS (99.86 mg/g) and AMMOP (99.86 mg/g) were recorded at pH 2; while the least for AMMOS (99.12 mg/g) and AMMOP (99.40 mg/g) were achieved at pH 10.

As shown in Figures 4, the amount of chromium adsorbed on the adsorbent increased with increase in concentration. The effect of the initial concentration factor depends on the immediate relation between the heavy metal concentration and the available binding sites on an adsorbent surface [23]. The optimum quantity of chromium adsorbed was found to be 301.553 mg/g and 398.961 mg/g for AMMOS and AMMOP respectively at a contact time of 60 minutes.

Results from this study shows that the adsorption capacity of both adsorbents AMMOS and AMMOP for the removal of chromium from the tannery effluent varies with temperature. The adsorption capacity increases to an optimum value within the temperature range of 10 - 50°C. At higher temperature, the chromium molecules are activated and the energy imparted to these adsorbates increases their mobility and thereby providing quicker access to the tan-chrome liquor interface. Secondly, the external mechanical agitation applied might have contributed in an increased permeation rate of the solute particles leading to increment in entropy of the system.

The adsorbent dosage Fig 5, determines the capacity of AMMOS or AMMOP for a given chromium concentration, which can also furnish the chromium-adsorbent equilibrium relations. Chromium uptake decreased with the increase in adsorbent loading (Figure 5) ranging from 0.01, 0.02, 0.03, 0.04 and 0.05 g for both AMMOS and AMMOP. This trend may be explained based on the mass balance relationship in Equation (2). At increasingly higher sorbent dosages (0.5 - 2.5 g), fixed initial chromium concentration (800 mg/L) and fixed aliquot volume (25 mL), the available chromium molecules are unable to cover all the exchangeable sites on the adsorbents, leading to decreased in chromium uptake at higher dosages. Chromium removal efficiencies expressed as a function of only the initial and final chromium concentrations, on the other hand, increased with increase in adsorbent dosage.

Adsorption isotherm studies

The relationship between the amount of a substance adsorbed per unit mass of adsorbent at a constant temperature and its concentration in the equilibrium solution is called adsorption isotherm. Adsorption isotherm is important to describe how solutes interact with sorbents. Developing an appropriate model for adsorption is essential to the design and optimization of adsorption processes. Data generated where fitted against four isotherm models namely; Langmuir, Freundlich, Temkin and Dubinin-Radushkevich.

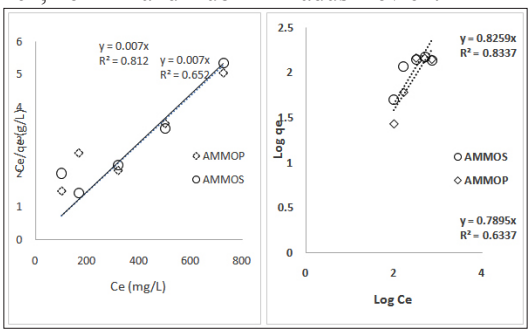

Figure 6: Langmuir (LHS) and Freundlich (RHS) isotherm plots of chromium adsorption on Acid modified MOS and MOP adsorbents

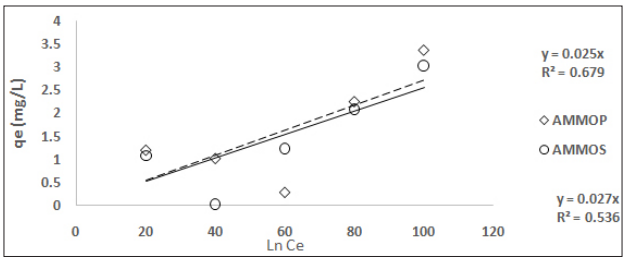

Figure 7: Temkin isotherm plot of chromium adsorption on Acid modified MOS and MOP adsorbents

Table 4: Isotherm Parameters for the Adsorption of Chromium ions onto the Adsorbents

Isotherms	Constant/ units	AMMOP	AMMOS
Langmuir	q_o	-1000	-333.3
	K_L	-0.0002	-0.001
	R_L	1.25	1.25
	R^2	0.6528	0.812
Freundlich	K_F (mg/g)	0.7895	0.8259
	1/n	0.88	1.39
	R^2	0.6485	0.8337
Temkin	b_T (kj/mol)	0.0272	0.0257
	K_T	0	0
	R_2	0.5364	0.6791
Dubinin-Radushkevich	q_s (mg/g)	1.1567	1.3229
	E	1.10	
	R_2	0.0637	0.0778

Langmuir isotherm

The equilibrium data for chromium over the concentration range 200 to 1000 mg/L respectively at 30°C has been correlated with the Langmuir isotherm (Figure 6). A linear plot was obtained when Ce/qe was plotted against Ce over the entire concentration range of chromium investigated. R^2 value of 0.271 for AMMOP and 0.7661 for AMMOS shows a good applicability of the model, indicating both monolayer adsorption and heterogeneous surface conditions. In Langmuir theory, the basic assumption is that the sorption takes place at specific homogeneous sites within the adsorbent. The essential feature of the Langmuir isotherm can be expressed by means of dimensionless constant separation factor (RL). RL value indicates the adsorption nature to be either unfavorable (RL> 1), linear (RL = 1), favorable (0 < RL < 1) or irreversible (RL = 0). In this context, lower RL value reflects that adsorption is more favorable. Result from this work shows adsorption is favorable for AMMOS than AMMOP (Table 4) which is in agreement with the report of Hameed and Foo, Result displayed showed AMMOS has a better applicability than AMMOP [24].

Freundlich isotherm

The equilibrium data for chromium over the concentration range of 200 to 1000 mg/L respectively at 30°C has been correlated with the Freundlich isotherm and the result is represented in (Figure 6) The sorption data is obeyed well. From the slope and intercept of straight portion of the plot. These values signify the sorption intensity and sorption capacity, respectively. The numerical value of n<1 indicates that bound sorbate molecules interact in such a

way that the binding strength is increased as more sorbate binds. Alternately, n>1 can mean that sorption capacity is only slightly suppressed at lower equilibrium concentration and suggests multiple binding sites, with the highest strength sites binding the sorbate first. The correlation coefficient values of Freundlich is given in Table 4 indicated that Freundlich was also a suitable correlation coefficient, (R^2) for AMMOS (0.8337), AMMOP (0.6485) adsorbent in chromium solution. The better fitting of these data into Freundlich isotherm than Langmiur shows that the adsorption of chromium onto AMMOS is an adsorption on a surface having heterogeneous energy distribution rather than monolayer sorption.

Temkin isotherm

The parameters given in Table 4 were obtained by plotting q_e vs In C_e. C_e is the equilibrium activities of heavy metal ions and q_e is the surface activity for chromium ions on the solid surface. The result was represented in Fig. 7. Correlation coefficient values of Temkin isotherm indicates that Temkin was the not suitable with a correlation coefficient, (R^2 of AMMOS (0.4005), AMMOP (0.3311) for the adsorbent in chromium solution.

Dubinin–Radushkevich isotherm

The Dubinin-Radushkevich isotherm parameters were obtained by plotting ln qe vs. E^2. The value of Ea is expected for physical adsorption. It is assumed to be heterogeneous in the structure of the adsorbents. The regression coefficient values R^2 show the applicability of the isotherms to the adsorption process.

Generally, the regression coefficient values of Langmuir, Freundlich, Temkin and Dubinin-Radushkevich models indicates that Temkin model was not suitable for any of the adsorbents but the three other models fitted for the adsorption processes. Correlation coefficient values of Dubinin-Radushkevich model indicates that Dubinin-Radushkevich is the least suitable isotherm for modeling Cr uptake on AMMOS (R^2 of 0.0778) and AMMOP (with R^2 value of 0.0637).

Adsorption Kinetic Studies

To investigate the rate of adsorption, the adsorbate (Cr) solution was brought in contact with the derived adsorbents at various contact times and the equilibrium data were modeled with kinetic models (Figure 8, Table 5). The adsorption of chromium over the adsorbents was practically completed in 1hour, showing the rapid adsorption of the heavy metals onto the adsorbents.

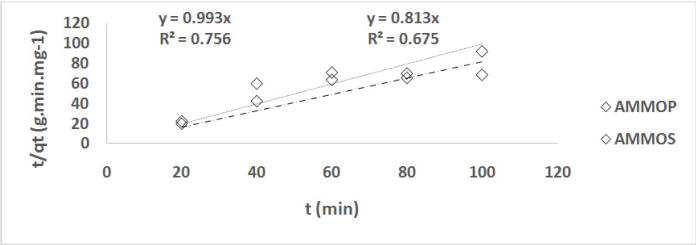

Figure 8: Plots of the pseudo-second-order kinetics of the chromium adsorption over AMMOS and AMMOP adsorbents

Table 5: Adsorption kinetic experimental parameters and constants

Kinetics models	Constants/units	AMMOP	AMMOS
Pseudo-First Order	q_e-exp (mg/g)	22.56	29.50
	K_1 (min^{-1})	0.015	0.016
	q_e-cal (mg/g)	66.66	62.50
	R^2	0.2824	0.7120
Pseudo-Second Order	qe-cal (mg/g)	158.38	16.07
	K_2 (g mg^{-1} min^{-1})	3.87 x 10^{-5}	5.76 x 10^{-6}
	R^2	0.6753	0.7566
Elovich	R^2	0.445	0.9438
	α (mg g^{-1} min^{-1})	0.3755	0.8432

The linearity of the second order kinetics for the adsorbents are relatively higher; AMMOS (0.7566), AMMOP (0.6753). Judging by the R^2 values of the plots on Table 5, pseudo-second order kinetic was proved to be effective in representing the experimental kinetic data for the adsorption having the higher R^2 value for most of the adsorbents. This suggests that the kinetics of chromium adsorption onto the adsorbents can be presented using the pseudo-second order model and hence suggests that chemical reaction might be responsible for the adsorption of heavy metals onto the adsorbents. Also for the pseudo-first order model, calculated values of the adsorption capacities qe, cal (mg/g) gave a better agreement with those of the experimental values qe, exp (mg/g) and the correlation coefficients R^2 is higher than those of the pseudo second order model.

Transport Studies

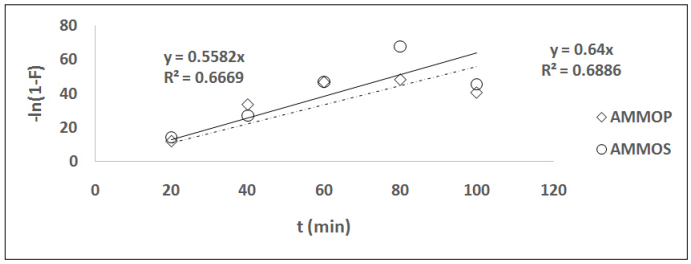

Figure 9: Film diffusion Plot for Chromium adsorption over acid modified MOS and MOPadsorbents

Table 6: Transport (Diffusion) Mode experimental constants

Transport models	Constants/ units	AMMOP	AMMOS
Intra-particle diffusion	R^2	0.534	0.5838
	K_{ID} (	0.015	0.016
	C_i (mg/L)	66.66	62.50
Film diffusion	q_e (cal)	158.38	16.07
	K_2	3.87 x 10^{-5}	5.76 x 10^{-6}
	R^2	0.6669	0.6886

Intra-particle diffusion model

It is obvious from the very low R^2 value for AMMOS (0.5838) and AMMOP (0.34) that the boundary layer has less significant effect about the diffusion mechanism of Cr uptake. The linear plot of qe vs. $t^{0.5}$ with intercept greater than zero indicates that intra-particle diffusion alone does not determine the overall rate of adsorption. The plots did not pass through origin indicating that the intra particle diffusion is not the only rate determining factor [25].

Film diffusion model

The liquid film diffusion model plots of ln (1-F) versus time was plotted for Cr and presented in Figure 9. The coefficient of regression (R^2) for AMMOS (0.5886); AMMOP (0.3869) was higher, implying that film diffusion could be the rate determining factor in the adsorption process. This model describes the movement of adsorbate across the external liquid film to the external surface sites on the adsorbent particle. The intercept values for both adsorbent are higher than zero, but close to the origin, confirming liquid film diffusion as the rate determinant of the adsorption process.

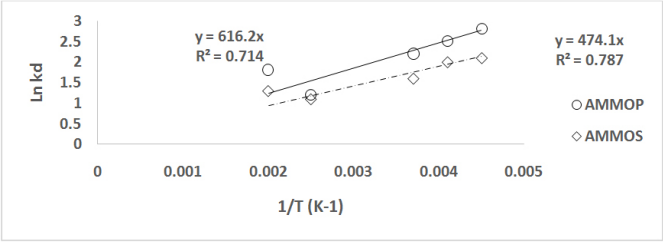

Figure 10: Van't Hoff Thermodynamic Plot for Cr Adsorption onto Acid modified MOS and MOP

Table 7: Thermodynamic experimental parameters and constants

Parameters	AMMOS	AMMOP
R^2	0.7873	0.7141
ΔS (kJ/mol)	2.2791	2.2662
ΔH (KJ/mol)	474.1	616.23
ΔG (KJ/mol.k)	471.8209	613.9638

Adsorption Thermodynamic Studies

It has been observed that with increase in temperature, adsorption capacity decreases. This implies that at the initial, the adsorption is exothermic in nature. The thermodynamic parameters change in Gibb's free energy (ΔGº), change in enthalpy ΔHº, and change in entropy ΔSº for the adsorption of Chromium over AMMOS, AMMOP was determined. The positive value for the enthalpy change, ΔH° for the adsorbents; AMMOS (474.1 kJ/mol) and AMMOP (616.23 kJ/mol) indicates the endothermic nature of the adsorption, which explains the increase of Chromium adsorption as the temperature increased until equilibrium is attained (Table 7). The positive value for the entropy change, ΔS° (2.2791 KJ/mol, 2.2662 KJ/mol, respectively), indicates that there is an increased disorder at the solid/liquid interface during Cr adsorption on the adsorbents. Free energy change (ΔG°) shows that the adsorption process of Chromium was exothermic and not spontaneous (A zraa et al., 2012).

Crystallographic parameters of the adsorbents

The crystallographic parameters for the adsorbents were presented for each adsorbent. The results (Tables 8 and 9) showed that AMMOS have 8 peaks, the 2θ ranging from 14.46 to 29.57 while AMMOP have 8 peaks too, the 2θ ranging from 13.47 to 3569.

Table 8: Crystallographic parameters AMMOS adsorbent

Peak position 2θ (degree)	Full width at half maximum intensity (FWHM) ß (rad)	d-spacing	Crystalline /D hkl size (um)
14.46	297.83	6.1188	0.00469
16.58	117.03	5.3415	0.0119
19.85	242.60	4.44692	0.00579
22.50	568.05	3.9479	0.00248
24.36	363.58	3.6503	0.00389
25.77	251.81	3.4543	0.00564
26.84	1000.00	3.3191	0.00142
29.57	124.92	3.0183	0.0114

Table 9: Crystallographic parameters AMMOP adsorbent

Peak position 2θ (degree)	Full width at half maximum intensity (FWHM) ß (rad)	d-spacing	Crystalline /D Hkl size (um)
13.47	100.21	6.5660	0.0139
14.37	132.55	6.1607	0.0105
17.45	879.76	5.0768	0.00159
20.21	459.49	4.3911	0.00306
22.33	692.24	3.9790	0.00204
27.45	1000.00	3.2462	0.00142
31.89	101.92	2.8041	0.0141
35.69	44.09	2.5137	0.0330

Test of significance and comparative Cr removal efficiency (% RE)

The effect of the several parametric factors were statistically tested and compared for significance at 95% confidence interval. Results are presented in (Table 10) compares the difference in perforbance by the derived adsorbents relative the different variables.

Table 10: Test of significance between Acid modified Moringa oleifera biomass

Experiment	Adsorbents	P-Values	Difference (P≥ 0.05)
Effect of initial concentration	AMMOS and AMMOP	1.000	Not significant
Effect of pH	AMMOS and AMMOP	.0091	Significant
Effect of Adsorbent Dosage	AMMOS and AMMOP	.009	Significant
Effect of Contact Time	AMMOS and AMMOP	.0089	Significant
Effect of Temperature	AMMOS and AMMOP	1.000	Not significant

Conclusion

Acid modified Moringa Oleifera seed shell and pod adsorbents prepared in this study showed favorable physicochemical characteristics and adsorptive behavior towards chromium removal from tannery effluent. The equilibrium chromium uptake was well modeled by the Langmuir isotherm. Adsorption kinetics obeyed the Pseudo-second-order kinetic model. The slow step is best explained by film diffusion model. Basic thermodynamic parameters

indicated that chromium uptake was feasible and exothermic for both adsorbents. The adsorbents may find potential use in the treatment of tannery effluents and wastewater [26,27].

References

1. Saleh TA, Gupta VK (2012b) Photo-catalyzed degradation of hazardous Dye Methyl orange by use of a composite catalyst consisting of multi walled carbon nanotubes and titanium dioxide. Journal of Colloids Interface Science 371: 101-106.
2. Demirbas E, Kobya M, Sulak MT (2008) Adsorption kinetics of a basic dye from aqueous solutions onto apricot stone activated carbon. Bioresources Technology 99: 5368-5373.
3. Ghaedi M, Sadeghian B, Pebdani AA, Sahraei R, Daneshfar A, et al. (2012) Kinetics, thermodynamics and equilibrium evaluation of direct yellow 12 removal by adsorption onto silver nanoparticles loaded activated carbon. Chemical Engineering Journal 187: 133-141.
4. Anjorin ST, Ikokoh PS, Okolo A (2010) Mineral composition of Moringaoleifera Leaves Pods and seeds from two regions in Abuja, Nigeria. International Journal of Agriculture and Biology 12: 1560-1569.
5. Lea M (2010) Bioremediation of Turbid Surface Water Using Seed Extract from Moringa oleifera Lam. (Drumstick) Tree. Current Protocols in Microbiology, 16, 1G.2.1-1G.2.14
6. Arafat MG, Mohamed SO (2013) Preliminary Study on Efficacy of Leaves, Seeds and Bark Extracts of Moringa oleifera in Reducing Bacterial load in Water. International Journal of Advanced Research 1: 124-130.
7. Reddy DHK, Harinath Y, Seshaiah K, Reddy AVR (2010) Biosorption of Pb (II) from aqueous solutions using chemically modified Moringa oleifera tree. Chemical Engineering Journal 162: 626-634.
8. Kansal SK, Kumari A (2014) Potential of M. oleifera for the treatment of water and wastewater. Chemical Reviews 114: 4993-5010.
9. Hsu R, Midcap S, Arbainsyah, De Witte L (2006) Moringa oleifera; medicinal and socioeconomic uses. International Course on Economic Botany, September 2006. National Herbarium, Leiden.
10. Ho SY, McKay G (1994) The kinetics of sorption of basic dyes from aqueous solution by Sphagnum moss peat. Canadian Journal of Chemical Engineering 76: 822-827.
11. Siddhuraju P, Becker K (2003) Antioxidant properties of various solvent extracts of total phenolic constituents from three different agroclimatic origins of drumstick tree (Moringa oleifera Lam) leaves. Journal of Agricultural Food Chemistry 51: 2144-2155.
12. Aslam MF, Anwar R, Nadeem U, Rashid TG, Kazi A, et al. (2005) Mineral composition of Moringa oleifera leaves and pods from different regions of Punjab, Pakistan. Asian Journal of Plant Science 4: 417-421.
13. Freeman N D IO, Pardon K K, Edison M, Mohammed B (2009) Characterisation of effluent from textile wet finishing operations. Proceedings of the World Congress on Engineering and Computer Science-WCEC (1), San Francisco, USA.
14. Wuana RA, Sha'A R, Iorhen S (2015a) Aqueous phase removal of norfloxacin using adsorbents from moringa oleifera pods husks, Advances in environmental research an international journal 4: 49-68.
15. Ahmedna M, Marshall WE, Rao RM (2000) "Production of granular activated carbon from selected agricultural byproducts", Bio-resource Technology 71: 113-123.
16. Toles CA, Marshall WE, Johns MM, Wartelle LA, McAloon A (2000) "Acid-activated carbons from almond shells: physical, chemical and adsorptive properties and estimated cost of production", Bioresource Technology 71: 87-92.
17. Gimba C, Musa I (2007) Preparation of activated carbon from agricultural waste: cyanide binding with activated carbon matrix from coconut shell. Journal of Chemical Nigeria 32: 167-170.
18. AWWA (1991) Standards for Granular Activated Carbons, American Water Works Association, ANSI/AWWA B604-90 Denver Co.
19. Mahmoud D K, Salleh MAM, Abdul Karim, WAW (2012) Characterization and evaluation agricultural solid wastes as adsorbents: A review", Journal of Purity, Utility Reaction Environment 1: 451-459.
20. Chen Xunjun (2015) Modelling of Experimental Adsorption Isotherm Data. Information 6: 14-22.
21. Yue Wen, Zhiru, Tang, Yi Chen, Yuexia Gu (2014) Adsorption of Cr (VI) from aqueous solutions using chitosan-coated fly ash composite as biosorbent Chemical Engineering Journal 175: 110-111.
22. Akhtar S, Qadeer R (2005) Kinetics Study of Lead ion Adsorption on active Carbon. Turkish Journal of Chemistry 29: 95-99.
23. Langmuir I (1918). The adsorption of gases on plane surfaces of glass, mica and platinum. Journal Am Chemical Sociology 40: 1361-1405.
24. Itodo AU, Abdulrahaman F W, Hassan L G, Maigandi S A, Hapiness U O (2011). Chemistry of pyrolysis and kinetic studies of Shea nut (Vitellariaparadoxa) shells activated carbon for textile eastern water treatment. Iranian Journal of Chemistry and Chemical Engineering 30: 51-57.
25. Itodo AU, Abdulrahman FW, Hassan LG, Maigandi SA, Itodo HU (2010). Physicochemical parameters of Adsorbents from locally sorted H3PO4 and ZnCl2 modified Agricultural wastes; New York Science Journal 3: 17-24.
26. Ajmal M, Rao RA, Ahmad K, Ahmad R (2000) Adsorption studies on Citrus reticulate (fruit peel of orange): removal and recovery of Ni (II) from electroplating wastewater. J. Hazard. Mater 79: 117-131.
27. APHA (American Public Health Association) (2005) Standard Methods for the Examination of Water and Wastewater (21ST Ed.) American Water Works Association, and Water Environment Federation, Washington DC.